Journal Pre-proofs

Original article

Polycyclic Aromatic Hydrocarbon and Soot Emissions in a Diesel Engine and from a Tube Reactor

Hamisu Adamu Dandajeh, Midhat Talibi, Nicos Ladommatos, Paul Hellier

PII: S1018-3639(20)30359-7
DOI: https://doi.org/10.1016/j.jksues.2020.12.007
Reference: JKSUES 471

To appear in: *Journal of King Saud University - Engineering Sciences*

Received Date: 3 June 2020
Accepted Date: 16 December 2020

Please cite this article as: Adamu Dandajeh, H., Talibi, M., Ladommatos, N., Hellier, P., Polycyclic Aromatic Hydrocarbon and Soot Emissions in a Diesel Engine and from a Tube Reactor, *Journal of King Saud University - Engineering Sciences* (2020), doi: https://doi.org/10.1016/j.jksues.2020.12.007

Polycyclic Aromatic Hydrocarbon and Soot Emissions in a Diesel Engine and from a Tube Reactor

Hamisu Adamu Dandajeh [1,2],* Midhat Talibi [2], Nicos Ladommatos [2] and Paul Hellier [2]
[1] Department of Mechanical Engineering, Ahmadu Bello University, Zaria PMB 1045, Nigeria
[2] Department of Mechanical Engineering, University College London, Torrington Place, London WC1E 7JE, UK

*[a]Corresponding Author: Hamisu Adamu Dandajeh. hamisu.dandajeh.14@ucl.ac.uk ; hadandajeh@abu.edu.ng

Polycyclic Aromatic Hydrocarbon and Soot Emissions in a Diesel Engine and from a Tube Reactor

Abstract

An investigation into the exhaust emissions of carcinogenic polycyclic aromatic hydrocarbons (PAHs) from a diesel engine was reported. The study is reinforced by the experimental results obtained from a tube reactor aimed at examining the PAH formation processes from these fuels. The paper cantered on the 16 priority PAHs suggested by the United States Environmental Protection Agency (US-EPA). These PAHs were produced by burning conventional diesel fuel and a few binary fuels prepared by blending various proportions of toluene into heptane. Special consideration was given to the B2 subgroup of PAHs which are known human-carcinogens. Both the gas born (smaller) PAHs, as well as the larger PAHs, adsorbed onto the particulate were investigated. The engine used was a single-cylinder, light duty, high speed, diesel automotive research engine run at an Indicated Mean effective pressure (IMEP) of 7bar. Particulate matter was also produced in a tube reactor at temperatures ranging from 1050 to 1350 °C under pyrolysis (oxygen-free) conditions to study PAH and soot formation in conditions which resemble, to an extent, those found in the core of diesel engine fuel sprays. In the diesel engine, it was found that exhaust PAHs were influenced by combustion characteristics like heat release rates and ignition delay. However, in the quiescent oxygen-free conditions of the reactor, chemical composition of the fuels and temperature dominated PAH formation.

Keywords: PAHs, soot, tube reactor, compression ignition engine, fuels

1.0 Introduction

Polycyclic Aromatic Hydrocarbons (PAHs) are probable human carcinogens and mutagens. Human mortality cases and other effects associated with soot bearing PAHs and several exhaust emissions have been reported (Dandajeh et al., 2017; Ismail and Umukoro, 2016). Petrogenic PAHs are found within the constituents of the fuels themselves while pyrogenic PAHs are generated during pyrolysis or combustion of hydrocarbon (Mcgrath et al., 2019). Production of pyrogenic PAHs is not only triggered by the prevailing conditions, but also by the medium in which the fuels are burnt (Dandajeh et al., 2019). For example, operating conditions and fuel type were reported to influence the emission of pyrogenic PAHs in the diesel engine (Borrás et al., 2009, Pedersen et al., 1980). In the tube reactor, however, pyrolytic conditions such as fuel concentration, residence time, temperature and the molecular structure of the fuel also affect pyrogenic PAH emissions (Sánchez et al., 2012). Studies on PAH emissions using a range of fuels are either done in diesel engine alone (Elghawi et al., 2010; He et al., 2010; Laroo et al., 2012), or individually in tube reactor (Dandajeh et al., 2018; Sánchez et al., 2012). Systematic comparative studies on PAH formation and emission in diesel engine and tube reactor using the same fuel molecule has rarely been studied. The extent to which soot particle toxicity is associated with PAHs from diesel engine and tube reactor is not well acknowledged. Moreover, it is still not known whether the emission of Group B2 PAHs from the diesel engines are comparable to those from the tube reactor.

This paper reports a comparative analysis of the PAH emissions from the tube reactor and diesel engine. The environment (high temperature and limited oxygen) that was employed in the tube reactor is broadly identical to that in the core of a diesel engine spray. The PAHs studied were the 16 PAHs listed in Table1 as compiled by the United State Environmental Protection Agency (US EPA), but the emphasis was accorded to the carcinogenic Group B2 PAHs. The PAH results from the reactor, where conditions were steady, controlled, laminar and homogenous are valuable for understanding the PAH results from the diesel engine where the conditions were more complex, unsteady, less controllable, extremely turbulent and heterogeneous.

Table 1: Priority list of 16 PAHs and their carcinogenic group (US, EPA, 1999)

Sn	PAHs	Carcinogenicity Group	Toxicity Factor	Molecular Weight (g/mole)	Number of Rings	Structure
1	Naphthalene	D	0.001	128	2	
2	Acenaphthylene	D	0.001	152	3	
3	Acenaphthene	NA	0.001	154	3	
4	Fluorene	D	0.001	166	3	
5	Phenanthrene	D	0.001	178	3	
6	Anthracene	D	0.01	178	3	
7	Fluoranthene	D	0.001	202	4	
8	Pyrene	NA	0.001	202	4	
9	Benzo[a]anthracene	B2	0.1	228	4	
10	Chrysene	B2	0.01	228	4	
11	Benzo[b]Fluoranthene	B2	0.1	252	5	
12	Benzo[k]Fluoranthene	B2	0.1	252	5	
13	Benzo(a)pyrene	B2	1.0	252	5	
14	Indeno[1,2,3-cd]pyrene	B2	0.1	276	6	
15	Dibenzo[a,h]anthracene	B2	1.0	278	5	
16	Benzo[g,h,i]perylene	D	0.01	276	6	

**Group B2 are PAHs that are possibly carcinogenic to humans and Group D are PAHs in which their carcinogenicity is not classified.*

2.0 Experimental

2.1 Test Fuels

The properties of the fuels tested are shown in Table 2. They are fossil diesel procured from Haltermann Carless, UK and heptane/toluene acquired from Sigma Aldrich also in the UK.

The diesel fuel had, on a mass basis, total aromatic contents of 22.2%. Heptane was selected as a surrogate fuel since its cetane number is close to that of the diesel fuel and its chemistry of PAHs is tractable. The volumetric proportions of toluene blended to heptane were 15% and 22.5%. This was used to mimic the range of aromatics in the reference fossil diesel

Table.2 Properties of test fuels (Hellier et al., 2013)

Fuel Properties	Diesel	Heptane	Toluene
H/C Ratio	1.771	2.28	1.143
Poly-aromatic hydrocarbon (% mass)	3.4%	-	-
Boiling Point(°C)	271.0[a]	98.3	110.6
Density (g/mL, 20 °C)	0.835	0.684	0.867
Cetane Number	52.7	54.4	7.4
Lower heating value (MJ/kg)	43.14	44.5	40.6

*[a] shows a point of 50% (by volume) recovery obtained according to ASTM D86 standard

2.2 Generation of Particulates

2.2.1 Diesel Engine

The engine used was a 4-stroke compression-ignition having a single-cylinder and has been described previously in (Dandajeh et al., 2019). Table 3 details the specifications while Figure 1 shows a schematic diagram of the engine assembly. The experimental facility consists of a fuel system under high pressure which was used to supply test fuels (heptane and heptane/toluene blends) to the fuel injector. The compartment of the fuel is made up of a stainless-steel vessel with a moveable piston and radial O-rings. The ends of the vessel were capped. The radial 'O-rings' divided the fuel vessel into two compartments. compartment 'A' contains diesel fuel while compartment 'B' houses the fuel to be tested.

Table 3: Engine Specifications

Description	Specification
Bore	86mm
Stroke	86 mm
Swept volume	499.56 cm3
Compression ratio (geometric)	18.3 : 1
Maximum in-cylinder pressure	150 bar
Piston design	Central (ω) bowl in piston
Fuel injection pump	Delphi single-cam radial-piston-pump
High pressure common rail	Delphi solenoid-controlled and pressure of 1600 bar max.
Diesel fuel injector	Delphi DFI 1.3 6-hole-solenoid-valve
Electronic fuel injection system	One micro-seconds (1µs) control duration
Crankshaft encoder	1800 pulse per revolution (ppr), 0.2 CAD resolution
Temperature of the Oil and coolant	80 ± 2.5 °C

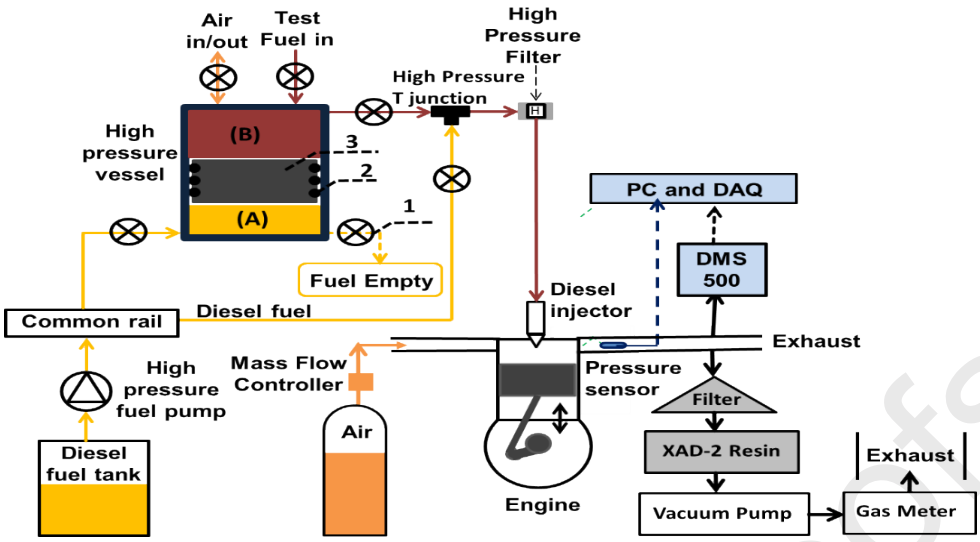

Fig.1 Engine Assembly Schematics showing sampling of the particulates and Gas phase PAHs '*1) high-pressure needle valve 2) 'O-ring' 3) moveable piston'*.

A pressurized diesel fuel was supplied to the fuel vessel via a conventional diesel fuel system. The pressurised diesel served as a hydraulic fluid that generated pressure in the test fuel via the free moving piston (see Fig.1). The radially installed 'O-rings' the piston's surface guaranteed no mixing of fuels between the two compartments. Emtronix system was used to pressurize the diesel fuel to a precise level. This pressure was transmitted to the test fuel via the free moving piston. The test fuel was injected at a common rail pressure of 450 bar. Experiments for all the fuels were conducted on the engine at a constant combustion phasing (constant engine speed of 1200rpm, the constant fuel injection pressure of 450bar and the constant start of fuel injection of 10 CAD (crank angle degrees) before the top dead centre. The injection duration was varied for all the experiments to maintain a constant IMEP of 7bar at the constant engine speed of 1200rpm. In the diesel engine, no lubricant additive was added to the fuel blends for the set experiments reported in this paper; hence no effect of the lubricant additive was noticed on the PAHs and particle emissions.

The test duration for each fuel and fuel blend was 15min. Engine fuel line was cleaned by combusting for 5minutes (without taking readings), the same fuel blend that will be burnt as the next available test fuel.

2.2.2 Tube Reactor

Soot and gaseous PAH samples were produced under oxygen-free pyrolysis at temperatures ranging from 1050 - 1350°C using a tube reactor previously Described in (Dandajeh, 2018). Figure 2 shows a schematic diagram of the experimental set-up. The carrier gas used was nitrogen at a constant flow rate of 20L/min using a mass flow controller. The fuel molecules were metered to the tube reactor at a constant carbon flow rate of 10,000ppm on C_1 basis. Each fuel was injected into a vaporizer system via a metered syringe pump, which was mechanically driven. All the hydrocarbon fuel blends, and the nitrogen carrier gas used during the pyrolysis were metered at standard temperature and pressure (STP) conditions. However, Proportional Integral Derivative (PID) controllers were used for monitoring and controlling both pressure and temperature during the experiments. The vaporizer was surrounded and heated by an electrical tape heater and then maintained at a temperature of 150°C by a proportional integral derivative (PID) controller.

As soon as the liquid fuel was injected into the hot nitrogen stream, the combined fuel and hot nitrogen stream passed into a static mixer. The static mixer ensured that the combined streams were mixed homogeneously.

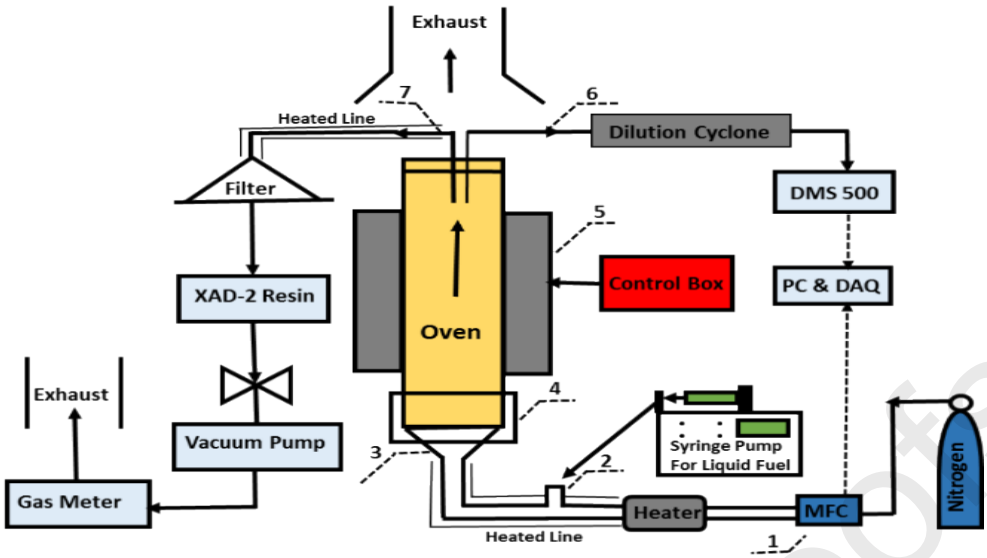

Fig.2: Schematics of the experimental facility: 1) mass flow controller (MFC) 2) fuel vaporizer 3) static mixer 4) circulating cooling water 5) tube furnace 6) DMS 500 sampling probe 7) soot sampling probe

The tube reactor was 1.44m long and its diameter was 0.104m. The alumina tube was situated vertically in an electric furnace (5) and about 0.6m of its length from the center was heated by the furnace. The heated section of the tube was maintained by an electrical PID controlled system at temperatures within the range of 1050 to 1350°C.

Table 4 summarized the differences in the physical conditions obtainable in both the tube reactor and the diesel engine as highlighted by Eveleigh et al., (2015).

Table 4: Prevailing conditions obtainable in the laminar tube reactor and the diesel engine (Eveleigh et al., 2015).

Tube Reactor	Diesel Engine
A homogenous mixture of fuel and air	Stratified
Fuel concentration of 10,000 ppm (C1 basis)	Overall fuel concentration of ~25,000 ppm
Conducted under pyrolytic conditions, and k = 0.1 and 0.2	Globally lean, stoichiometric in a combustion regions, rich spray core
Temperature 1350°C	Calculated maximum global in-cylinder Temperature ~1000°C; flame temperature ~2000 °C
Laminar and controllable	Turbulent and less controllable
Residence time ~1 s	Duration of combustion ~ 0.008 s. Residence time (fuel injection to the end of exhaust stroke) ~ 0.05 s
Atmospheric pressure	Variable pressure, with a peak pressure of ~60 bar

2.3 Sampling of PAHs and Particulates

2.3.1 Diesel Engine

Characteristics of the particulates in the exhaust of the diesel engine were known using a DMS-500 (Cambustion) differential mobility spectrometer. The DMS-500 gives real-time outputs of particle mass, number and size. The exhaust stream was sampled about 300mm downstream of the engine exhaust valves. The gas stream was transported to the particulate analyzer via a heated line maintained at a temperature of 80°C. Soot particles were sampled at 40 L/min at about 1000mm downstream of the engine exhaust using a stainless-steel probe of half-inch diameter. The probe was connected to a vacuum-pump. Particulate filter (glass micro-fibre, 70mm diameter, 0.7µm pore size) was used to collect particulates. The filter, which was procured from Fisher Scientific, UK, was first desiccator-dried for 12 hours. The filter was initially weighed before sampling on a high precision mass balance. The balance has deviation of ± 0.001mg. The filter, after sampling, was desiccator-dried again for another 12hours and then re-weighed. The particulate-mass collected on the filter was measured. The particulate filter in the high-temperature engine exhaust was protected by sandwiching it between two stainless steel wire meshes. The wire meshes were cut to the same diameter as the filter. The filter was sandwiched to avoid its deterioration. The filter had 0.026mm aperture, 0.025mm wire diameter and was procured from the mesh company, UK.

The stainless-steel resin-based system was used to trap gaseous PAHs. The gas-volume that passed through the particulate-filter and the resin (in series) was measured using a volumetric gas meter. The meter was procured from Bell flow Systems, UK. Detailed of the sampling procedure can be found in Dandajeh et al., (2017). Two samples of both the particulates and gas-phase PAHs were collected for each test fuel and the average readings were recorded and shown in Table 5. The soot mass concentration was found by diving the particulate mass by the recorded volume of gas.

2.3.2 Tube Reactor

The soot sampling probe (7) was heated by a tape heater and controlled by a PID controller at a temperature of 120°C to avoid condensation of gaseous PAHs. Soot particles that were generated within the reactor were sampled from the outlet of the reactor using a half-inch stainless-steel probe. The probe was serially connected to a vacuum pump. A control valve maintained the flow rate of the vacuum pump, always at < 18 L/min. A gas flow meter was used to measure the volume of gas that passed through the particulate filter and the XAD-2 resin. The particulate system and the XAD-2 resin were connected in series. The same soot collection system that was used in the engine experiment was also used in the tube reactor. The gravimetric filter mass measurements and calculated soot mass concentration from the fuel pyrolysis are depicted in Table6.

2.4 Sample Preparation

Sample preparation involves sample extraction and subsequent solvent evaporation. The extraction of PAH species from the soot and resin samples generated from both the diesel engine and tube reactor was implemented via an accelerated solvent extractor (ASE) (Thermo Scientific Dionex-150). ASE is a technique for automatically extracting PAHs at high pressure and temperature and it is approved by the US EPA for PAH extraction (Richter et al., 1996). Both the soot and resin samples were extracted using a dichloromethane solvent. since, it was used previously for PAH recoveries (Dandajeh et al., 2018). The extraction conditions were a temperature of 125°C and pressure of 100bar. All extractions were carried out using a 10mL sample/solvent cell, purge time of 60secs and rinse volume of 40% under one static cycle. Extraction of each sample was repeated three times in a single collection vial, which made the total accumulated volume of the extracts to 6omL. Sample concentration/solvent evaporation was carried out by gently bubbling a nitrogen stream at 5L/min through the extraction vial containing the PAH-extracts. The collection vial containing the 60mL extracts was in a PID controlled stainless steel heating mantle. The 60mL extracts were first concentrated to < 15mL and later transferred a graduated glass tube was concentrated further to 1mL.

2.5 GC-MS Analysis

The 1mL final concentrated volume of each extract was analyzed using Agilent gas chromatograph (7890B GC) coupled to a mass spectrometer (5977A MSD). The GC column used was an HP-5 (30m x 250µm x 0.25µm) with helium as a carrier gas at a flow rate of 1.2L/min. The injection mode was split-less, injecting 1µL of each sample using an automatic liquid sampler (ALS) at a temperature

of 300°C. Heating of the GC oven started with a temperature of 50°C, held for 1min. This was followed by a heating rate of 25°C/min increased to 150°C, held for another 1min. The further heating rate of 25°C/min increased the temperature to 200°C and was held for 1min. Additional heating rate of 3°C/min increased the temperature to 230°C and was held for 1min. Lastly, a heating rate of 8°C/min raised the temperature to 310 °C and was held for 3 min. Each sample was run on the GC for 33.0 minutes. The temperature of the transfer line, MS Source, and MS quad were 290°C, 230°C and, 150°C respectively. Single quadrupole was used as the MS in electron ionization (EI) mode.

Before PAH quantification, the GC was calibrated using standard reference material **(47930-U SUPELCO)** (Sigma Aldrich, UK). The reference material consisted of 16 US EPA PAHs which are already shown in Table1. Detailed calibration of the GC-MS is explained in Dandajeh et al., (2017).

3.0 Results and Discussion

3.1 Soot Formation in Diesel Engine and Tube Reactor

This section presents soot formation during combustion and pyrolysis of fuels in diesel engine and tube reactor respectively. Fig.3a shows the apparent heat release rates for pure heptane (100%H0%T), 85%heptane15%toluene (85%H15%T) and 77.5%heptane22.5%toluene (77.5%H22.5%T). In Figure 3, Diesel start and Diesel finish are readings for diesel fuel combustion at the start and the end of each daily tests respectively. It can be seen from Fig.3a that H85%T15% blend, having an ignition delay of 9.8 crank angle degree (CAD), exhibited the highest heat release rate relative to the reference fossil diesel fuel (both start and finish) and pure heptane. The binary mixtures of 77.5%H22.5%T exhibited the second-highest heat release rate, but with the longest ignition delay of 10.8 CAD. Increasing ignition-delay (ID) duration due to increase in the volume of toluene blended into heptane was reported previously by Hellier et al. (2013), who researched binary mixtures of heptane/toluene blends in a direct injection compression ignition engine.

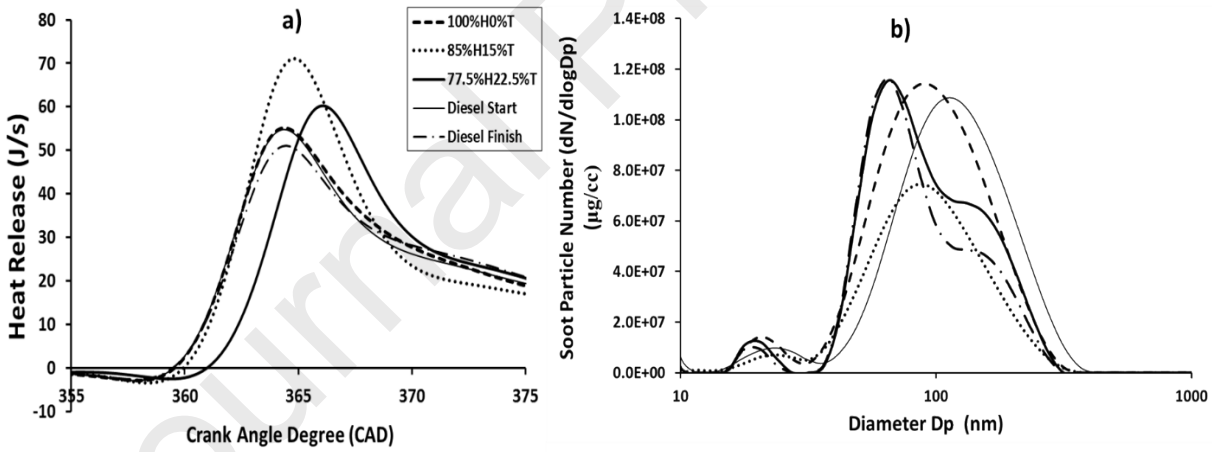

Fig.3: a) Heat release rate (J/deg) b) Soot particle number concentration (dN/dlogDp) (µg/cc)

The reference fossil diesel-start and pure 100%H0%T exhibited the same heat release rates and ignition delay of 9.4 CAD. This was also reported in previous studies (Hellier et al., 2013), and is expected since both the reference fossil diesel and 100%H0%T have close cetane numbers and lower heating values (see Table 2). However, the reference diesel run at the end of the daily test series exhibited slightly lower heat release rates, 4J/s lower than that of the diesel start. This test to test variations was largely due to the daily drift in the engine.

Fig.3b shows the soot particle number concentrations of all the fuels tested measured in the diesel engine exhaust using DMS500 particle spectrometer. It can be seen from Fig.3b that the sizes of the soot particle for all the test fuels in diesel engine ranged from 30 – 360nm. The mean

size and surface area (μm²/cm³) of the soot particles for each the fuel tested are shown in Table 5.

Table 5 showed that blending toluene to heptane increased soot particle sizes. These particle sizes increased from 176.1nm for 100%H to 177.8nm and 181.3nm for 85%H15%T and 77.5%H22.5%T respectively. The gravimetric filter measurements shown in Table 5 were also confirmed from those measured using DMS500 instrument. It is obvious from Table 5 that the concentration of the soot mass increased from 39 – 45mg/m³ by changing the fuel blend from 85%H15%T and 77.5%H22.5%T. It should be mention here that the soot mass concentration of 100%H0%T was unanticipatedly high and one should be cautious in interpreting this result, considering the daily variations in the soot concentrations in the engine.

Table 6 shows the mass of soot particles gotten by filter measurements which resulted from the pyrolysis of both pure heptane and 85%H15%T. It can be seen from Table 6 that temperature increase also increased soot mass concentrations of both 100%H0%T and 85%H15%T blend. Pyrolysis of n-heptane was reported to be attributed to the abundance of C_2- C_6 radicals such as acetylene and propargyl radicals (Ding et al., 2013) which are mostly contributory in the making the first-aromatic-ring (Richter and Howard, 2000). However, blending 15% of toluene into heptane increased the calculated soot mass concentration by 10.6 times at a temperature of 1050°C, 2.25 times at 1150 °C, 1.54 times at 1250°C and 1.69 at 1350°C. Some backing to this finding from the literature is the study of Alexiou and Williams, (1995), who found decreasing propensity of toluene soot in reflected shock-tube pyrolysis when heptane was blended into it. This is not surprising since, firstly; toluene is a prolific sooter because its nucleation rates increase exponentially with temperature (Dandajeh et al., 2019).

Table 5: Gravimetric soot mass (filter measurements) from the diesel engine

Fuel	soot mass (mg)	Soot concentration (mg/m³)	mean soot particle diameter (nm)	soot surface area (μm²/cm³)
100%H0%T	23.0	48.0	176.1	2720005
85%H15%T	19.25	39.9	177.8	1647524
77.5% H22.5%T	23.5	45.0	181.3	2367265
Diesel	28.7	58.0	186.6	1846044

Table 6: Gravimetric soot mass (filter measurements) from the tube reactor

	100% H0%T		**85%H15%T**	
Temperature (°C)	Soot (mg)	Soot Conc. (mg/m³)	Soot (mg)	Soot Conc. (mg/m³)
1050	7.500	20.325	85.20±3.7	215.70±53.2
1150	72.80	362.20	149.8	814.13
1250	133.7	726.63	189.4	1120.7
1350	116.5	658.20	184.8±3.2	1113.3±5.0

Secondly, toluene pyrolysis is also associated with the abundance of C_2 - C_6 radicals including acetylene, propargyl and phenyl radicals (Zhang et al., 2010), and blending it into heptane could increase the number of these radicals which would serve as soot precursors. Furthermore, the fact that toluene is a valuable source of phenyl-radicals via its de-methylation could trigger PAH growth by phenyl-addition and cyclization (PAC) (Shukla et al., 2008) and consequently, increase soot propensity of the heptane/toluene blend. The

increased presence of acetylene in pyrolysis of toluene could trigger PAH production. Frenklach, (2002) explained this using hydrogen-abstraction, acetylene, addition (HACA). Ladommatos et al. (1996) also reported toluene producing soot by at least 18.5 times than heptane in a diffusion flame. Based on the foregoing, it can, therefore, be deduced that while combustion characteristics had more influence on the concentration of soot formed in diesel engine, temperature and chemical composition of the fuels pyrolyzed had the greatest effects on soot formation in the case of tube reactor.

3.2 Total PAH analysis in Diesel Engine

Fig.3 shows the total gas-phase (GP) and particle-phase (PP) PAH concentration, which emerged by adding up all the 16 US-EPA-PAHs produced by burning each fuel. PAH concentrations were either normalized by the gas- volume (m^3) passed serially through a particulate filter and XAD-2 resin or by the mass of soot collected (mg). Fig.3a shows the total GP-PAH concentration which was 1906 $\mu g/m^3$ for 100%H0%T. This PAH mass decreased to 1336 $\mu g/m^3$ and 1067 $\mu g/m^3$ when 85%H15%T and 77.5H22.5%T were respectively burnt. These results suggest that the amount of toluene added to heptane combustion was inversely proportional to the GP PAHs generated during the combustion of the fuel. This is because toluene addition into heptane promoted soot formation. Hence, more carbon in the heptane/toluene blends is converted to soot and less carbon is available as PAHs. Some support for this explanation appeared in Fig.3b. It can be seen from Fig.3b that the amount of toluene added to heptane does not only increase the concentration of soot particles generated, it also increased the PAH mass concentration on the particulates. For example, in 100%H0%T, the concentration of PP PAHs was 60$\mu g/m^3$ and it increased by 48% for 85%H15%T and 67% for 77.5%H22.5%T. The particle phase PAHs in diesel fuel was found to be higher than the 100%H0%T and all the heptane/toluene blends. This is consistent with previous studies (Barbella et al., 1989).

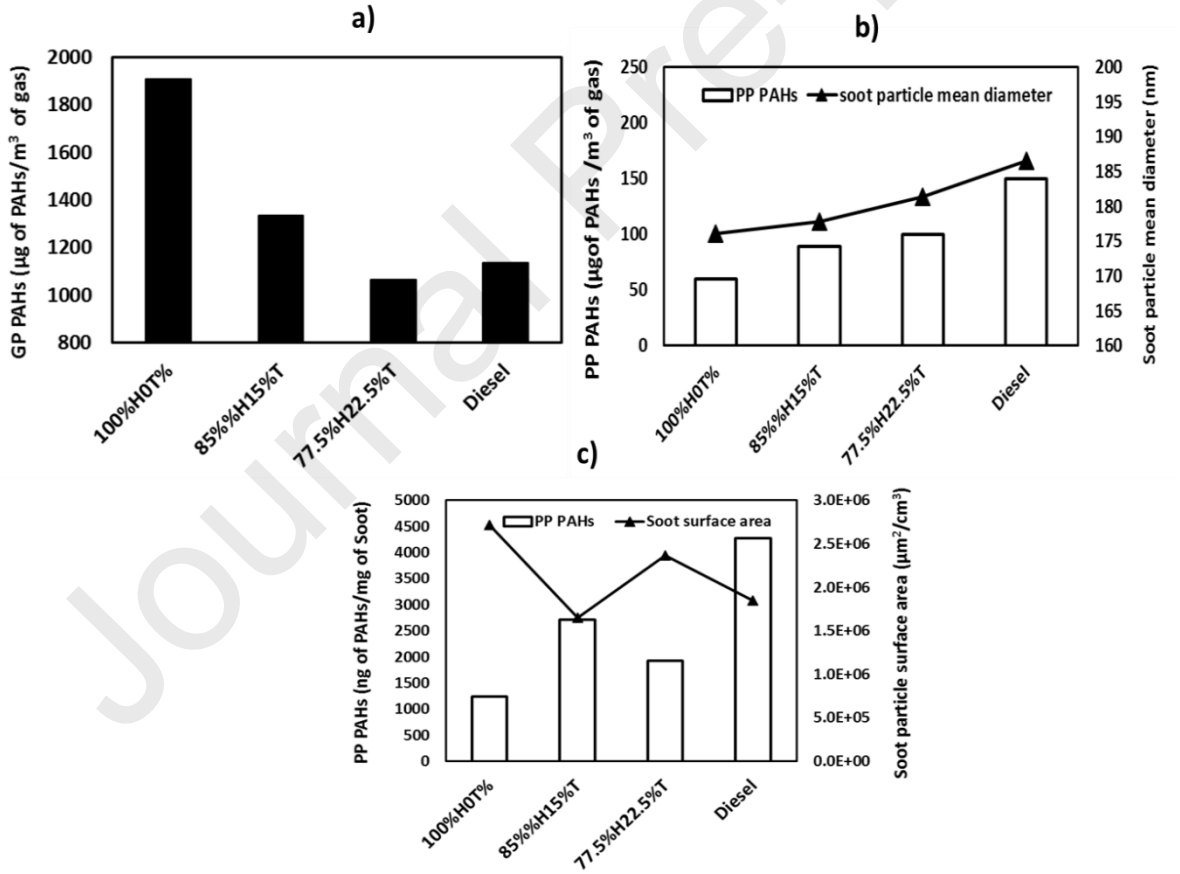

Fig. 3: Total PAHs in diesel engine: a) Gas Phase (normalised by m^3 of gas) and soot particle mean diameter (nm) b) Particle Phase (normalised by m^3 of gas) c) Particle Phase (normalised by mg of soot) and particle surface area ($\mu m^2/cm^3$)

The correlation between the particle phase PAHs and their corresponding mean diameter of soot particles from which the PAHs were extracted is also shown in Fig.3b. The figure shows a direct relationship between the concentration of PAHs and soot particle size. It is therefore apparent from Fig.3b that adding toluene to heptane also aided increasing the sizes of soot-particles onto which the PAHs are attached. Fig.3c shows the mass of PAHs on the soot particles generated from all the fuels normalized with the mass of soot particle generated by the combustion of each fuel.

3.3 Total PAH analysis in Tube Reactor

Fig.4a and b show the total PAH concentrations from the tube reactor in the gas and particulate phases respectively. It is evident from Fig.4a that, the concentrations of GP PAHs dropped with temperature rise from 1050 - 1350°C for all the fuels pyrolyzed. This results corresponds with those of Sánchez et al., (2012), who studied PAH emissions on gaseous fuels. The 85%H15%T blend was higher in concentration at all temperatures tested. Fig.4b showed a similar trend for the heptane/toluene blend with those in Fig.4a, but with 100%H0%T having a slightly different trend. The PP PAH for 100%H0%T in Fig.4b showed an increase in concentration with temperature rise from 1050 - 1150°C, the concentration peaked at 1150°C and then decreased with temperature increase from 1150 -1350°C. The peaking of PP PAH concentration of pure heptane at the temperature of 1150°C and subsequent decrease with rising a temperature possibly suggest a competition for PAH production and their resulting consumption in soot formation. Font et al. (2003) also reported this tendency of sharp increase and decrease of PP PAH concentrations in polyethylene pyrolysis, but at slightly lower temperature.

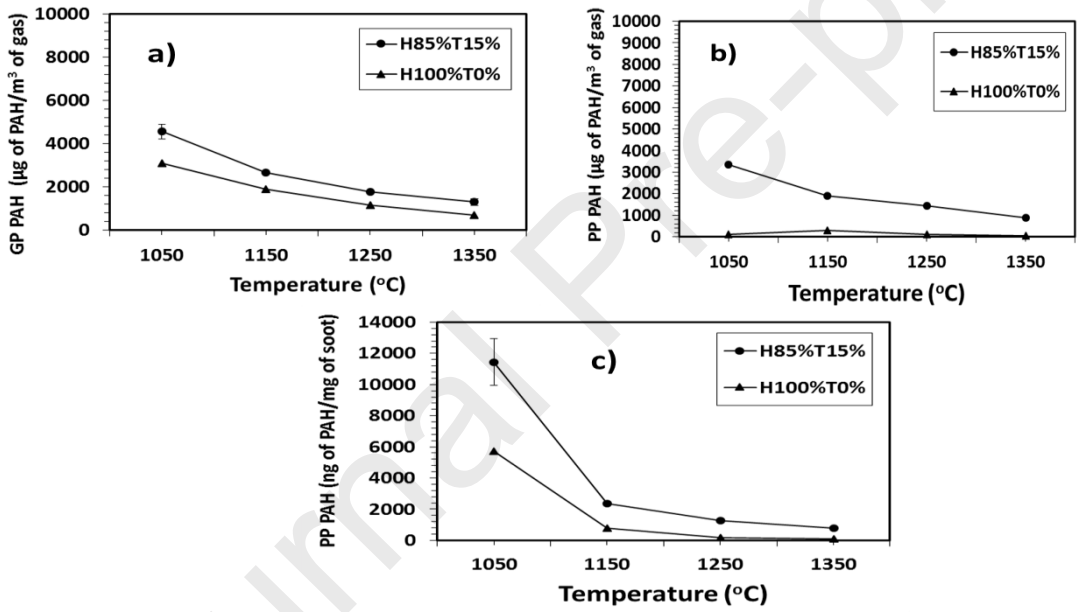

Fig.4: Total PAHs in a tube reactor: a) Gas Phase (normalised by m³ of gas) b) Particle Phase (normalised by m³ of gas) c) Particle Phase (normalised by mg of soot)

Fig.4c shows the PP PAH concentrations per unit soot-mass. It is evident from the figure that, at the low temperature of 1050 °C, both 100%H0%T and 85%H15%T blend showed higher PAH mass concentrations. The PP PAH concentrations of both fuels decreased markedly when the temperature was raised to 1150 °C. The PAH mass concentrations further decrease when the temperature was raised to 1350 °C. It The decrease in PP PAH mass concentrations with a rise in temperature could be associated with the corresponding increase in the soot mass concentrations generated from the pyrolysis of the fuels tested (see Table 6). Taking a closer look at Fig.4 in its entirety, one could observe that the fuel effect on the GP and PP PAH mass concentrations in the tube reactor was more pronounced at the lowest temperature of 1050°C. However, the fuel effect had less effect on PAH emissions when the temperature was raised to 1350 °C.

3.4 Proportions of gaseous and particle phase PAHs

Fig.5a shows the proportions of gas-phase (GP) and particle-phase (PP) PAHs in the diesel engine and tube reactor. It is clear from Fig.5a that diesel

engine combustion is influenced by the GP PAHs irrespective of the fuel tested. For instance, the GP PAH proportion generated while combusting 100%H0%T was 97% and this decreased to 94% for 85%H15%T and 91% for 77.5%H22.5%T. However, only 88% of the GP PAHs were while combusting diesel fuel. This result of GP PAHs dominating the total PAHs agreed with previous works (Sánchez et al., 2013).

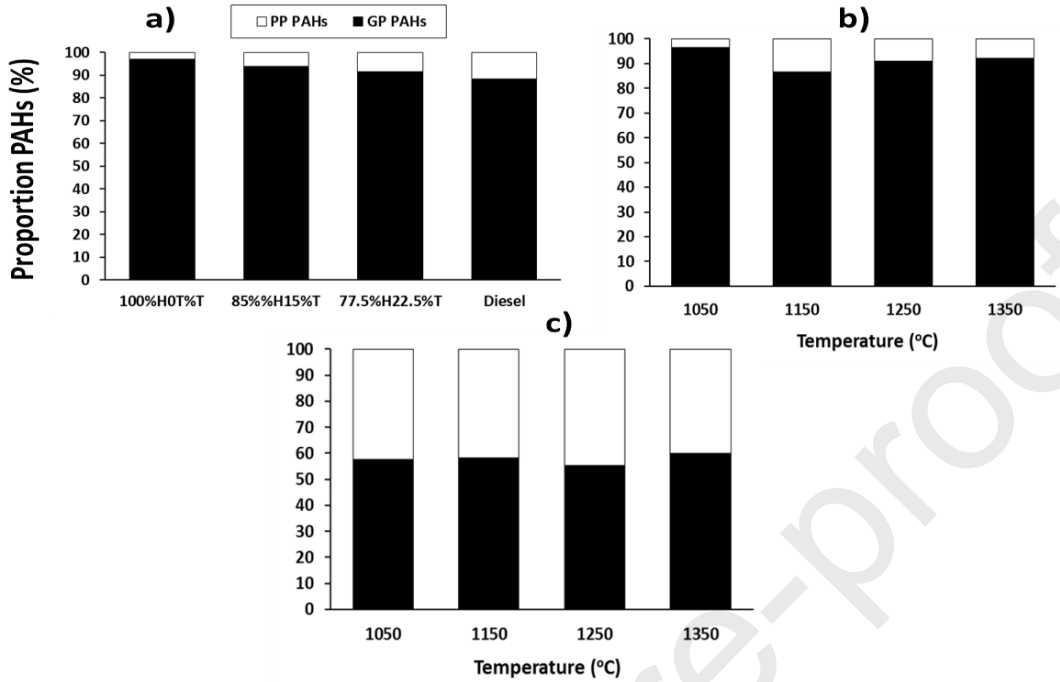

Fig. 5: Proportions of gas-phase and particle phase PAH distributions a) Engine b) 100%H0%T (tube reactor) c) 85%H15%T (tube reactor).

Fig.5b and Fig.5c show the proportions of GP and PP PAHs pyrolysis of pure heptane and 85%H15%T respectively in the tube reactor. It can be observed from Fig.5b that the proportions of GP PAHs in the total PAHs decreased while that of PP increased with the rise in temperature. For example, the PP increased from 3.6% at temperature of 1050°C to 13.3% when the temperature was increased to 1150°C. However, Fig.5c shows that when the 85%H15%T blend was pyrolyzed, the proportion of PP increased considerably by 42% at the temperature of 1050°C and was found to be somewhat insensitive with temperature rise.

3.5 Toxicity of Soot Particles

The results for the Group B2 PAHs extracted from the soot masses generated from the fuels tested, as well as their carcinogenicity are presented in this section. Table 7 shows the sum of the Group B2 PAHs in diesel engine and their respective proportions in the total PAHs. It can be seen from Table 7 that the proportion of the Group B2 PAHs for the fossil diesel was 40.9% in the particle phase and 12.7% in the total PAHs. The high proportions of PAHs on the soot particles generated from fossil diesel is expected, since, its combustion was associated with a substantial soot mass concentration (58 mg/m^3) when compared with other fuels tested. However, the percentage of the Group B2 PAHs deposited on the soot particles from the various heptane/toluene blends increased from 22.2% for the 100%H0%T, peaked at 30.4% for 85%H15%T and decreased to 12.1% for 77.5%H22.5%T.

Table 7: Sum of Group B2 PAHs and their proportions in total PAHs in diesel engine

	ΣGroup B2 in PP PAHs (µg/m3)	ΣGroupB2/ ΣPP PAHs (%)	ΣGroup B2 in Total PAHs (µg/m3)	ΣGroupB2/ Total PAHs (%)

100%H0%T	13.28	22.2	99.49	5.1
85%%H15%T	27.13	30.4	58.59	4.1
77.5%H22.5%T	12.08	12.1	47.08	4.03
Diesel	61.20	40.9	163.26	12.7

The trend in the Group B2 PAHs for the heptane/toluene blends is like those in the apparent heat release rates. In Fig.3a for example, the heat release rates increased from 54J/s for pure heptane, peaked at 71J/s for 85%H15%T and decreased to 59J/s for the 77.5%H22.5%T. This suggest that the formation of Group B2 PAHs in diesel engine combustion might be affected by the heat release rates. Furthermore, the Group B2 PAHs do not increase linearly with the proportions of toluene added to heptane, they instead decreased beyond 15%toluene blended into heptane. While the above statement could be conjectured, the formation of soot, Group B2 PAHs and the corresponding WC-PAHs, as reported earlier by Dandajeh, (2018), depends remarkably on how much heptane/toluene blend is burned during the premixed combustion, mixing controlled combustion and late combustion. It is important to note that the accuracy and reliability of the experimental data are dependent the error margins shown in Table 8

Table8: Percentage Variations (100% δ /mean) for the test parameters investigated

Parameter	**Percent Variation (±%)**
Soot concentration, Ms/Vg (±mg/m3)	18
Peak heat release rates (±J/s)	2.4
Peak in-cylinder pressure (±bar)	0.7
Particle Number, dN/dDp (±1/cm3)	15
GP PAHs (±µg of PAH/m3 of gas)	17
PP PAHs (±µg of PAH/m3 of gas)	29
PP PAHs (±ng of PAH/mg of soot)	0.2
Total PAHs (±µg of PAH/m3 of gas)	19

The PAH weighted-carcinogenicty (WC-PAHs) was stated by Dandajeh et al. (2018) as summing the product of concentration (C_n) for each of the 16 EPA PAH and their toxic equivalent factor (TEF_n). The relation on the WC-PAHs is as shown in equation 1. The toxic equivalence factors of PAHs used in this work are those shown in Table 1 and were first introduced by Nisbet and LaGoy in (1992).

$$\text{WC-PAHs} = \sum_{n=1}^{16}(TEF_n * C_n) \quad 1)$$

Fig.6 shows the weighted carcinogenicity of soot particles for the tube reactor and diesel engine. Fig.6a and 6b show, respectively, the WC- PAHs of pure heptane and 85%H15%T in the tube reactor on a volume of gas and mass of soot bases. One can see from Fig.6a that the WC- PAHs for 100%H0%T was 20 µg/m^3 at a temperature of 1050°C, but it increased 12 times when 85%H15%T blend was pyrolyzed. One reason why the WC-PAH was higher for the 85%H15%T blend was that its pyrolysis generated soot particles with substantial concentrations (C_n) of benzo(a)pyrene and diben(a,h)anthracene, both of which have a TEF of unity.

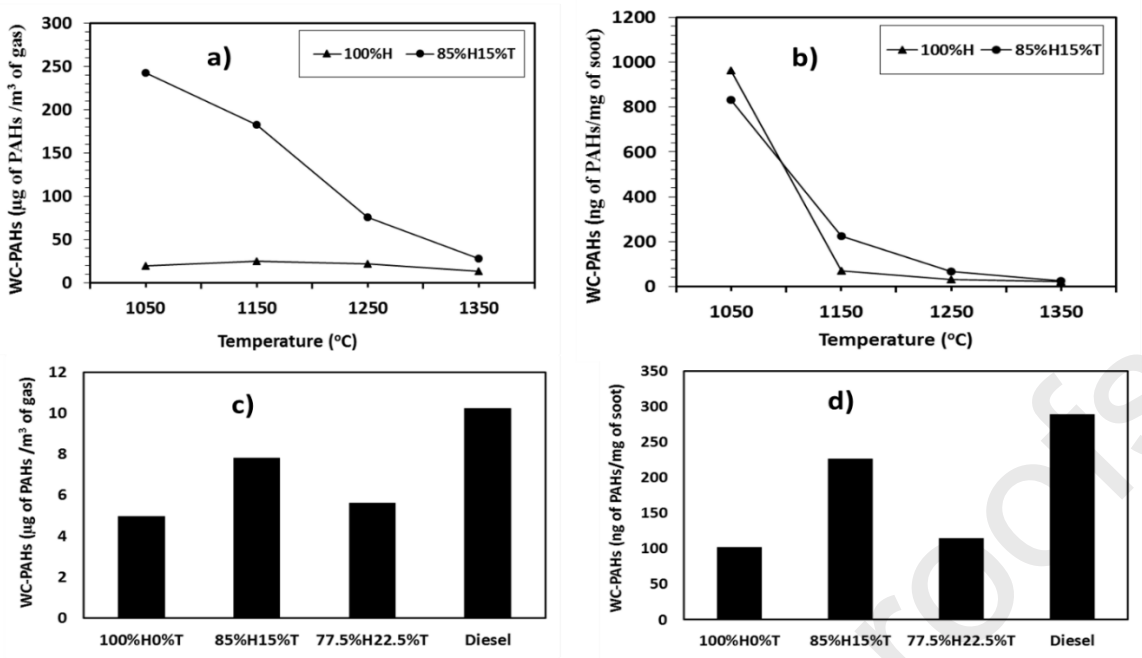

Fig.6: Normalised Weighted Carcinogenicity of particle-phase PAHs a) & b) in tube reactor c) & d) in diesel engine

It is also apparent that WC-PAHs of the 85%H15%T blend decreased remarkably when the temperature was increased from 1050 -1350°C but remained remarkably higher at all temperatures than 100%H0%T. Consider now Fig.6b, the WC-PAHs (soot mass basis) of both 100%H0%T and 85%H15%T blend also peaked a temperature 1050 °C and remarkably when the temperature was raised from 1050 – 1150°C. The WC-PAHs was somewhat independent on temperature, within the range of 1150 -1350°C

Fig.6c and Fig.6d show the WC-PAHs from the diesel engine on a volume of gas basis and soot mass basis respectively. It can be seen from both figures that the WC-PAHs for all the fuels tested reflect the particle phase PAH concentrations of the B2 subgroup shown in Table 7. The evidence from this result suggests that the WC-PAHs of the heptane/toluene blends are also influenced by their heat release rates shown in Fig.3a.

4.0 Conclusions

Results of PAHs extracted from both gaseous and particulate phases are presented. These PAHs were generated by pyrolyzing and combusting diesel and blends of heptane/toluene fuels in a diesel engine and in a tube reactor respectively. From the results of this study, the following conclusions can be made:

1) In diesel engine, where combustion conditions are turbulent and less controllable, the gas phase PAHs controlled the total PAH concentrations (> 90%) irrespective of the nature of fuel burnt. The proportion of the gas phase PAHs decreased with increasing toluene proportion in heptane. Diesel fuel had the lowest proportions of PAHs in the gas phase of 88%, but the highest proportions of PAHs in the particulate phase.

2) In the tube reactor where pyrolysis conditions are laminar and controllable, the gas phase PAHs also controlled the total PAH concentrations, but at 4% lesser than that in the diesel engine. This dominance of GP PAHs was temperature-dependent in the case of 100%H0%T and was almost insensitive to temperature (~ 55%) for 85%H15%T.

3) Blending toluene into heptane in both diesel engine and the tube reactor, did not only increase the PAHs in the particulate phase, it also increased the sizes of the soot particles in which the PAHs are deposited.

4) Heat release rates in the diesel engine while combusting the test fuels may have influence not only on the concentrations of the amount of soot formed and the GroupB2 PAHs on the particulates and their weighted-carcinogenicity values.

5) In the tube reactor, the chemical composition of the fuel had the strong influence at the lowest temperature of 1050°C and this effect was seen to gradually diminish at higher temperatures of 1350°C.

Acknowledgements

The first author wishes to gratefully acknowledge the Petroleum Technology Development Fund (PTDF) for sponsoring his research studies at University College London (UCL).

Conflict of Interest

The authors declare no conflict of interest

References

Alexiou, A., Williams, A., 1995. A. Alexiou and A. Williams 74, 153–158.

Barbella, R., Ciajolo, A., Anna, A.D., 1989. Effect of Fuel Aromaticity on Diesel Emissions 277, 267–277.

Borrás, E., Tortajada-Genaro, L. a., Vázquez, M., Zielinska, B., 2009. Polycyclic aromatic hydrocarbon exhaust emissions from different reformulated diesel fuels and engine operating conditions. Atmos. Environ. 43, 5944–5952. https://doi.org/10.1016/j.atmosenv.2009.08.010

Dandajeh, H.A., 2018. Effect of molecular structure of liquid and gaseous fuels on the formation and emission of PAHs and soot 1–230. PhD Thesis Submitted to the University College London.

Dandajeh, H.A., Ladommatos, N., Hellier, P., Eveleigh, A., 2018. In fl uence of carbon number of C 1 – C 7 hydrocarbons on PAH formation 228, 140–151. https://doi.org/10.1016/j.fuel.2018.04.133

Dandajeh, H.A., Ladommatos, N., Hellier, P., Eveleigh, A., 2017. Effects of unsaturation of C2 and C3 hydrocarbons on the formation of PAHs and on the toxicity of soot particles. Fuel 194, 306–320. https://doi.org/10.1016/j.fuel.2017.01.015

Dandajeh, H.A., Talibi, M., Ladommatos, N., Hellier, P., 2019. Influence of Combustion Characteristics and Fuel Composition on Exhaust PAHs in a Compression.

Ding, J., He, G., Zhang, L., 2013. Detailed Temperature-dependent Study of n-Heptane Pyrolysis at High Temperature. Chinese J. Chem. Phys. 26, 329. https://doi.org/10.1063/1674-0068/26/03/329-336

Elghawi, U.M., Mayouf, a., Tsolakis, a., Wyszynski, M.L., 2010. Vapour-phase and particulate-bound PAHs profile generated by a (SI/HCCI) engine from a winter grade commercial gasoline fuel. Fuel 89, 2019–2025. https://doi.org/10.1016/j.fuel.2010.01.002

EPA Method TO, 1999. Method TO-13A: Compendium of Methods for the Determination of Toxic Organic Compounds in Ambient Air Second Edition Compendium Method TO-13A Determination of Polycyclic Aromatic Hydrocarbons (PAHs) in Ambient Air Using Gas Chromatography / Mass Spectrom. Epa.

Eveleigh, A., Ladommatos, N., Hellier, P., Jourdan, A., 2015. An investigation into the conversion of specific carbon atoms in oleic acid and methyl oleate to particulate matter in a diesel engine and tube reactor. Fuel 153, 604–611. https://doi.org/10.1016/j.fuel.2015.03.037

Font, R., Aracil, I., Fullana, A., Martín-Gullón, I., Conesa, J. a., 2003. Semivolatile compounds in pyrolysis of polyethylene. J. Anal. Appl. Pyrolysis 68–69, 599–611. https://doi.org/10.1016/S0165-2370(03)00038-X

Frenklach, M., 2002. Reaction mechanism of soot formation in flames. Phys. Chem. Chem. Phys. 4, 2028–2037. https://doi.org/10.1039/b110045a

He, C., Ge, Y., Tan, J., You, K., Han, X., Wang, J., 2010. Characteristics of polycyclic aromatic hydrocarbons emissions of diesel engine fueled with biodiesel and diesel. Fuel 89, 2040–2046. https://doi.org/10.1016/j.fuel.2010.03.014

Hellier, P., Ladommatos, N., Allan, R., Rogerson, J., 2013. Combustion and emissions characteristics of toluene/n-heptane and 1-octene/n-octane binary mixtures in a direct injection compression ignition engine. Combust. Flame 160, 2141–2158. https://doi.org/10.1016/j.combustflame.2013.04.016

Ismail, O.S., Umukoro, G.E., 2016. Modelling combustion reactions for gas flaring and its resulting emissions 130–140.

Ladommatos, N., Rubenstein, P., Bennett, P., 1996. Some effects of molecular structure of single hydrocarbons on sooting tendency. Fuel 75, 114–124. https://doi.org/10.1016/0016-2361(94)00251-7

Laroo, C. a., Schenk, C.R., Sanchez, L.J., McDonald, J., Smith, P.L., 2012. Emissions of PCDD/Fs, PCBs, and PAHs from legacy on-road heavy-duty diesel engines. Chemosphere 89, 1287–1294. https://doi.org/10.1016/j.chemosphere.2012.05.022

Mcgrath, J.A., Joshua, N., Bess, A.S., Parkerton, T.F., 2019. Review of Polycyclic Aromatic Hydrocarbons (PAHs) Sediment Quality Guidelines for the Protection of Benthic Life 15, 505–518. https://doi.org/10.1002/ieam.4142

Nisbet, I.C.T., LaGoy, P.K., 1992. Toxic equivalency factors (TEFs) for polycyclic aromatic hydrocarbons (PAHs). Regul. Toxicol. Pharmacol. 16, 290–300. https://doi.org/10.1016/0273-2300(92)90009-X

Pedersen, P.S., Ingwersen, J., Nielsen, T., Larsen, E., 1980. Effects of fuel, lubricant, and engine operating parameters on the emission of polycyclic aromatic hydrocarbons. Environ. Sci. Technol. 14, 71–79. https://doi.org/10.1021/es60161a011

Richter, B.E., Jones, B. a, Ezzell, J.L., Porter, N.L., 1996. Accelerated Solvent Extraction : A Technique for Sample Preparation. Anal. Chem. 68, 1033–1039. https://doi.org/10.1021/ac9508199

Richter, H., Howard, J.., 2000. Formation of polycyclic aromatic hydrocarbons and their growth to soot—a review of chemical reaction pathways, Progress in Energy and Combustion Science. https://doi.org/10.1016/S0360-1285(00)00009-5

Sánchez, N.E., Callejas, a., Millera, a., Bilbao, R., Alzueta, M.U., 2012. Formation of PAH and soot during acetylene pyrolysis at different gas residence times and reaction temperatures. Energy 43, 30–36. https://doi.org/10.1016/j.energy.2011.12.009

Sánchez, N.E., Millera, Á., Bilbao, R., Alzueta, M.U., 2013. Polycyclic aromatic hydrocarbons (PAH), soot and light gases formed in the pyrolysis of acetylene at different temperatures: Effect of fuel concentration. J. Anal. Appl. Pyrolysis 103, 126–133. https://doi.org/10.1016/j.jaap.2012.10.027

Shukla, B., Susa, A., Miyoshi, A., Koshi, M., 2008. Role of phenyl radicals in the growth of polycyclic aromatic hydrocarbons. J. Phys. Chem. A 112, 2362–9. https://doi.org/10.1021/jp7098398

Zhang, L., Cai, J., Zhang, T., Qi, F., 2010. Kinetic modeling study of toluene pyrolysis at low pressure. Combust. Flame 157, 1686–1697. https://doi.org/10.1016/j.combustflame.2010.04.002